


BRIEF REPORT

Open Access



Ablation of Siglec-E augments brain inflammation and ischemic injury

Lexiao Li^{1†}, Yu Chen^{1†}, Madison N. Sluter¹, Ruida Hou¹, Jiukuan Hao², Yin Wu³, Guo-Yun Chen³, Ying Yu¹ and Jianxiong Jiang^{1*} 

Abstract

Sialic acid immunoglobulin-like lectin E (Siglec-E) is a subtype of pattern recognition receptors found on the surface of myeloid cells and functions as a key immunosuppressive checkpoint molecule. The engagement between Siglec-E and the ligand $\alpha_{2,8}$ -linked disialyl glycans activates the immunoreceptor tyrosine-based inhibitory motif (ITIM) in its intracellular domain, mitigating the potential risk of autoimmunity amid innate immune attacks on parasites, bacteria, and carcinoma. Recent studies suggest that Siglec-E is also expressed in the CNS, particularly microglia, the brain-resident immune cells. However, the functions of Siglec-E in brain inflammation and injuries under many neurological conditions largely remain elusive. In this study, we first revealed an anti-inflammatory role for Siglec-E in lipopolysaccharide (LPS)-triggered microglial activation. We then found that Siglec-E was induced within the brain by systemic treatment with LPS in mice in a dose-dependent manner, while its ablation exacerbated hippocampal reactive microgliosis in LPS-treated animals. The genetic deficiency of Siglec-E also aggravated oxygen–glucose deprivation (OGD)-induced neuronal death in mouse primary cortical cultures containing both neurons and glial cells. Moreover, Siglec-E expression in ipsilateral brain tissues was substantially induced following middle cerebral artery occlusion (MCAO). Lastly, the neurological deficits and brain infarcts were augmented in Siglec-E knockout mice after moderate MCAO when compared to wild-type animals. Collectively, our findings suggest that the endogenous inducible Siglec-E plays crucial anti-inflammatory and neuroprotective roles following ischemic stroke, and thus might underlie an intrinsic mechanism of resolution of inflammation and self-repair in the brain.

Keywords: Cerebral ischemia, DAMPs, Infarct, Innate immunity, LPS, Microgliosis, Neuroprotection, OGD, PAMPs, Sialic acid

Introduction

Sialic acids are a group of monosaccharides with a nine-carbon backbone and are most commonly represented by *N*-acetylneuraminic acid (Neu5Ac) and *N*-glycolylneuraminic acid (Neu5Gc). The $\alpha_{2,8}$ or $\alpha_{2,3}$ -linked oligopolymers or polymers by this subtype of monosaccharides

construct the terminal decoration of the glycocalyx located on the cell surface. These sialoglycan structures serve as specific “identity code” ligands of host cells and are recognizable for corresponding membrane receptors of immune cells. This set of immunorecognition-involved receptors are referred to as sialic acid-binding immunoglobulin-type lectins or Siglecs. By far, 15 members of Siglecs have been identified in humans and nine in mice. They overall can be divided into two subfamilies: conserved Siglecs that can be found in different mammals and CD33-related Siglecs which do not have clear orthologs across species but rather functional paralogs (e.g., Siglec-9 and Siglec-E) [1]. The selective *trans*- and

[†]Lexiao Li and Yu Chen contributed equally to this work.

*Correspondence: jjiang18@uthsc.edu

¹ Department of Pharmaceutical Sciences, Drug Discovery Center, College of Pharmacy, University of Tennessee Health Science Center, Memphis, TN, USA

Full list of author information is available at the end of the article



cis-binding between ligands and receptors leads to the activation of motifs in the intracellular domains, and the downstream signaling cascades are implicated in immunomodulation. Depending on those intracellular motifs, the immunomodulatory property of a specific Siglec can be inhibitory or stimulatory. Most Siglecs are inhibitory because they carry the immunoreceptor tyrosine-based inhibitory motif (ITIM) or ITIM-like domains. The others contain a positively charged amino acid residue in the transmembrane domain that enables their binding to DAP12 (also known as KARAP or TYROBP) that has an activating intracellular immunoreceptor tyrosine-based activation motif (ITAM) [2, 3]. As such, Siglecs regulate immune checkpoint mechanisms and are thought to mitigate the risk of autoimmunity amid innate immune attacks on parasites, bacteria, and carcinoma.

Siglec-E is one of the most representative members in mouse CD33-related Siglec subfamily. As a pattern recognition receptor located on the surface of myeloid cells, Siglec-E functions as a key immunosuppressive checkpoint molecule. The engagement between Siglec-E and the ligand $\alpha_{2,8}$ -linked disialyl glycans activates the ITIM located in its intracellular domain. Since Siglec-E was first cloned about two decades ago [4], it has been extensively studied in a wide range of conditions, such as carcinoma [5–11], parasite infection [12–15], bacterial infection and sepsis [16–22], inflammatory lung diseases [23–25], chronic obstructive pulmonary disease [26], asthma [27, 28], atherosclerosis [29], hyperglycemia and diabetes [30, 31], and autoimmune diseases [32]. Siglec-E has also been widely found within the brain, particularly activated microglia [33, 34]; however, its functions in neuroimmune system remain largely unknown.

Accounting for about 5–15% of all cells in the CNS, microglia are widely recognized as the resident myeloid cells in the brain parenchyma and play essential roles in brain homeostasis and innate immunity [35]. As such, the reactive microgliosis is an intense reaction of microglia to inflammatory stimuli, such as exogenous pathogen-associated molecular patterns (PAMPs) and endogenous damage-associated molecular patterns (DAMPs), and is primarily featured by rapid, robust and sustained increases in activated microglia at the sites of brain insults. Given that microglia are the major cell type expressing Siglec-E within the brain, the functions of microglial Siglec-E have recently been studied in neuroinflammation-associated conditions. Activation of Siglec-E by microglia-derived polysialic acid ligands was shown to inhibit the inflammatory responses to lipopolysaccharide (LPS) stimulation in microglial cell line BV2 and to traumatic brain injury (TBI) in mice [34]. Likewise, interaction between microglial Siglec-E and sialic acids likely serves as a sensitive immune checkpoint axis and

might underlie a molecular mechanism whereby anti-tumor immunity in glioma patients with steroid therapies is compromised [8]. To date, however, there is no study reported to investigate the role of microglial Siglec-E in brain inflammation and injury following ischemic stroke, a world-wide leading cause of death and adult disability.

Acute cerebral ischemia causes the primary brain injury mainly due to the malfunction of energy metabolism and neuronal excitotoxicity, while reactive microgliosis-associated neuroinflammatory processes induced by post-ischemic necrosis largely contribute to the delayed, secondary injury [36]. Understanding the molecular mechanisms underlying the post-stroke neuroinflammation and secondary injury is essential to the development of immunomodulatory therapies for ischemic stroke [37, 38]. In the present study, we investigated the effects of congenital ablation of Siglec-E in mouse primary microglia activated by LPS and in mouse cortical cultures subjected to oxygen–glucose deprivation (OGD). We also studied the roles of Siglec-E in the activation and morphological alterations of brain microglia in mice treated by LPS. Further, we examined the outcomes, such as neurological deficits, weight changes, and brain infarcts, in Siglec-E knockout mice after middle cerebral artery occlusion (MCAO). We propose that the elevated Siglec-E activity in microglia by ischemic injury alleviates the neuroinflammatory reactions and protects neurons from the subsequent escalated injuries, and thus might represent an intrinsic mechanism for inflammation resolution and brain tissue self-repair after cerebral ischemia.

Methods

Mouse primary microglial cultures

The mouse primary microglial cultures were prepared as we previously described [39, 40]. Briefly, cortical tissues were isolated from newborn C57BL/6 mouse pups (P1) and were dissected in ice-cold Hank's balanced salt solution (HBSS, Corning). Meninges and blood vessels were carefully removed. After repeated gentle trituration, filtration was performed to separate cells from tissue debris and chunks. The cells were then cultured in minimum essential medium (MEM) supplemented with 10% fetal bovine serum (FBS), 100 U/mL penicillin, and 100 μ g/mL streptomycin in 0.001% poly-L-ornithine-coated flasks. Four to 5 days later, fresh complete MEM plus 2 ng/mL granulocyte–macrophage colony-stimulating factor (GM-CSF) was loaded (R&D Systems). After incubation for additional 4–5 days, matured microglia were collected by gentle agitation of the culture flasks. The harvested microglia were seeded into 48-well plates with fresh complete MEM plus 0.2 ng/mL GM-CSF (4×10^4 cells/well). Such mouse primary cultures typically consisted of at least 95% Iba1-positive (Iba1⁺) cells

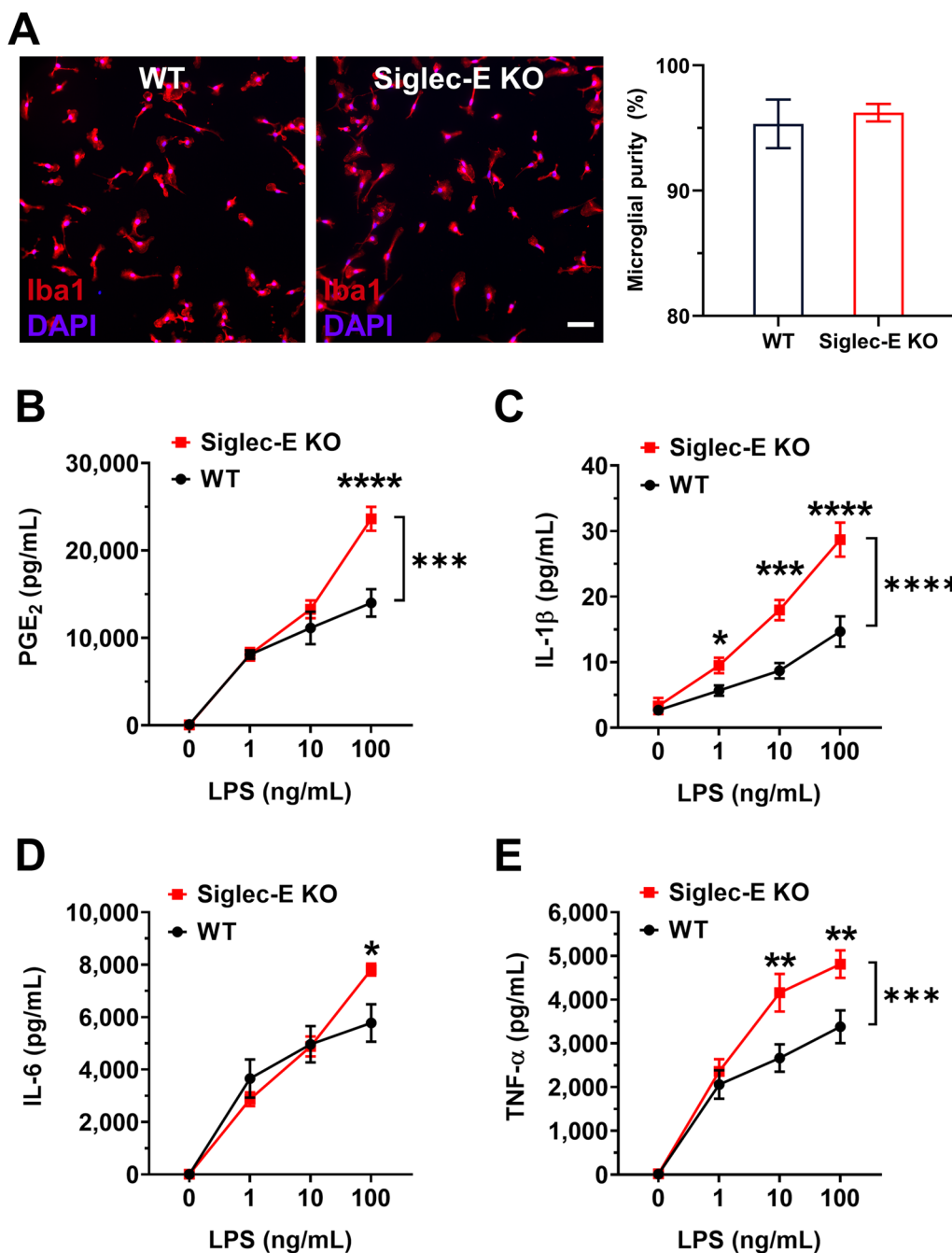


Fig. 1 Siglec-E suppresses prototypical proinflammatory mediators in LPS-activated microglia. **A** Mouse primary brain microglia from C57BL/6 wild type and Siglec-E knockout pups were prepared in 48-well plates (4×10^4 cells/well). The purity of microglia in these cultures was assessed by immunostaining for the microglial marker Iba-1 (red fluorescence) and compared ($n = 9$, $p = 0.678$, Mann-Whitney U test). Note that cell nuclei were stained with DAPI (blue fluorescence) to illustrate all cell types. Scale bar: $50 \mu\text{m}$. The cultured cells were then stimulated with LPS (0, 1, 10, or 100 ng/mL) for 16 h. A number of key proinflammatory mediators that were secreted by LPS-activated microglia into the culture medium, such as PGE₂ (**B**), IL-1β (**C**), IL-6 (**D**), and TNF-α (**E**), were measured by ELISA. Note that all these conventional proinflammatory mediators produced by microglia were induced by LPS treatment in a concentration-dependent manner and were further dramatically increased in the absence of Siglec-E ($n = 8-12$, $*p < 0.05$; $**p < 0.01$; $***p < 0.001$; $****p < 0.0001$, two-way ANOVA with post hoc Šidák multiple comparisons). All data are presented as mean \pm SEM

as identified by immunocytochemistry (Fig. 1A). To stimulate microglia, these primary cultures were incubated with lipopolysaccharide (LPS) at concentrations ranging from 1 to 100 ng/mL overnight. ELISA was used to measure the conventional proinflammatory mediators in the cultural medium, including prostaglandin E₂ (PGE₂), interleukin 1 β (IL-1 β), IL-6, and tumor necrosis factor α (TNF- α). The manufacturers' protocols in the ELISA kits were followed as we previously described [40].

Mouse primary cortical cultures

Cortical cells were isolated from embryos (E18) of timed-pregnant C57BL6 mice as we previously described [41, 42]. Cells were seeded into poly-D-lysine (Sigma-Aldrich) coated 24-well plates (~300,000 cells/well) and cultured at 37 °C in a humidified incubator supplied with 5% CO₂ and 95% air. Cells were cultured in neurobasal medium supplemented with B-27, sodium pyruvate, dextrose, L-glutamine, 100 U/mL penicillin, and 100 μ g/mL streptomycin (Invitrogen). Half of the culture medium was replaced by fresh medium every 3–4 days, and immunocytochemistry confirmed that these cultures consisted of neurons, microglia, and astrocytes. On 10–14 days in vitro, these mouse primary neuron–glia mixed cortical cultures were subjected to oxygen–glucose deprivation (OGD) stress as we previously described [40, 43]. In brief, primary cells were incubated in glucose/glutamate-free DMEM (Gibco), and the culture plates were then sealed in a vacuum bag. The hypoxic condition was achieved through continuous aspiration by a vacuum pump which decreased the air pressure in the vacuum bag to 0.079 standard atmosphere and reduced the oxygen level to about 1.66% [40].

Experimental animals

All animal experiments and procedures were approved by the Institutional Animal Care and Use Committee (IACUC) of the University of Tennessee Health Science Center and performed in line with the *Guide for the Care and Use of Laboratory Animals* (the *Guide*) from the National Institutes of Health (NIH). Mice were housed in standard humidity (45–50%) at room temperature (21–25 °C) under a 12-h light/dark cycle with ad libitum access to food and water. Siglec-E knockout mice were from the Mutant Mouse Regional Resource & Research Center (MMRRC_032571-UCD). Siglec-E gene in 129/Sv ES cells underwent targeted mutations, and the Siglec-E knockout mice were generated with the mutated 129/Sv ES cells. These mice were backcrossed to the C57BL/6 background for over eight generations to reduce the impact of 129-derived passenger gene mutations [17, 22, 44]. The wild-type littermates were used as controls for Siglec-E knockout mice.

Mouse model of transient brain ischemia

Acute focal brain ischemia was prepared using middle cerebral artery occlusion (MCAO) as we previously described [40, 41, 45]. Buprenorphine SR-LAB (1.0 mg/kg, s.c.) for analgesia was given 1 h before the surgery. Mice were anesthetized via inhalation of vaporized isoflurane (Henry Schein) at 1.5–2%. The rectal temperature was monitored via a digital thermometer and was maintained at 37 °C using a heating pad. With an incision made on neck skin along the midline, soft tissues were gently separated to expose the vessel field on the right side. The vagal nerve was carefully dissociated from the common carotid artery, and the superior thyroid artery was ablated before the ligation of external carotid artery (ECA). The ECA was then cut off using a cauterizer (Bovie Medical Corporation). The occipital artery located above the CCA bifurcation was carefully ablated before the internal carotid artery (ICA) and pterygopalatine artery (PPA) became visible. The CCA and ICA were clamped with microvascular clips. With a 5-0 suture knot loosely prepared at the root of ECA, a tiny nick was made along the ECA stump for the insertion of the filament into ECA lumen. MCAO was achieved through delivering a 20-mm-long 6-0 silicon-coated Doccol filament into ICA by 10 mm to cease the blood supply into MCA. The properly placed filament was fixed by tightening the loose knot at the root of ECA. During the MCAO session, mice were placed above another heating pad for the restoration of consciousness. Thirty minutes later, reperfusion was started by withdrawing the Doccol filament. The researcher who performed this surgery had no knowledge about the genotype of mice. Successful MCAO surgery should result in marked neurological deficits. The assessment of post-stroke neurological deficits was performed also in a blinded manner as we previously described [40, 41]. The scoring scale was modified from Bederson's and Longa's versions as follows: 0, no deficit; 1, forelimb flexion; 2, reduced resistance to lateral push; 3, unidirectional circling; 4, barrel rolling/spinning; 5, no movement.

Quantification of infarct and edema

Three days after reperfusion from MCAO, mice were euthanized under overdosed isoflurane anesthesia and subjected to transcardial perfusion with icy phosphate-buffered saline (PBS). A mouse coronal brain matrix was employed to help the preparation of 1-mm-thick coronal brain sections. These sections were stained with 0.2% TTC solution (2,3,5-triphenyltetrazolium chloride, Santa Cruz Biotechnology) for 20 min, aligned, and captured for digital imaging and analysis. The infarct size was quantified using ImageJ/Fiji

software (NIH) in a blinded manner. The sum of infarct volume was performed following the stereological principle. The infarct volume was further adjusted based on the ipsilateral edema size in compliance with “Swanson’s correction”. The adjusted infarct volume was finally normalized to its contralateral brain volume in order to offset any artifactual impact including physical extension and shrinkage during the tissue processing.

LPS model of brain inflammation

LPS from *Escherichia coli* O111:B4 was purchased from Sigma-Aldrich. For injection, LPS was dissolved in sterile isotonic saline and injected to mice with a volume of 10 mL/kg. Eight-weeks-old male C57BL/6 mice were weighed and randomized to treatments with LPS (3 or 5 mg/kg, i.p.) or saline [46]. Twenty-four hours after LPS injection, mice were anesthetized with isoflurane, then perfused with ice-cold PBS. Brain tissues were dissected and collected for biochemical and immunohistochemical analyses.

Quantitative PCR

The total RNA from mouse brain tissues was extracted using the combination of TRIzol (Invitrogen), chloroform, and the PureLink RNA Mini Kit (Invitrogen). The purity and concentration of extractant were measured via the readings of A260/A280 ratio and A260, respectively, by a NanoDrop One microvolume spectrophotometer (Thermo Fisher). The single-stranded complementary DNA (cDNA) was synthesized using the SuperScript III First-Strand Synthesis SuperMix (Invitrogen) following the manual. The quantitative PCR (qPCR) was performed using 8 μ l of 10 \times diluted cDNA, 0.4 μ M of primers and 2 \times SYBR Green SuperMix (Bio-Rad Laboratories) with a final volume of 20 μ l in a CFX96 Touch Real-Time PCR Detection System (Bio-Rad Laboratories). The cycling protocols were set as: 95 $^{\circ}$ C for 2 min followed by 40 cycles of 95 $^{\circ}$ C for 15 s and then 60 $^{\circ}$ C for 1 min. The fluorescent readings were set at the 60 $^{\circ}$ C step. Melting curve procedure was added to verify the uniformity of PCR product. The cycle of quantification for GAPDH gene was subtracted from the cycle of quantification measured for each gene of interest to yield Δ Cq [40, 42]. Samples without cDNA template served as negative controls. The sequences of primers for qPCR were as follows: GAPDH, forward 5'-TGTCCGTCGTGGATCTGAC-3' and reverse 5'-CCTGCTTACCACCTTCTTG-3'; Siglec-E, forward 5'-GTCTCCACAGAGCAGTGC AACTTTATC-3' and reverse 5'-TGGGATTCAAC AGGGGATTCTGAG-3'.

Immunofluorescence staining

Immunostaining was performed as we previously reported [47, 48]. In brief, fixed coronal brain section (25 μ m) underwent 60-min permeabilization and blocking with PBS containing 0.2% Triton X-100, 10% goat serum, and 22.52 mg/mL glycine. The sections were then incubated in rabbit anti-Iba1 polyclonal antibody (Wako cat. #019-19741, 1:200) and rat anti-Siglec-E monoclonal antibody (BioLegend cat. #677102, 1:100) at 4 $^{\circ}$ C overnight. Slices were then rinsed and incubated with anti-rabbit and anti-rat secondary antibodies conjugated with Alexa Fluor 546 or 488 (1:1000, Invitrogen) for 2 h. The slices were carefully mounted onto slides using the ProLongTM Gold antifade reagent (Invitrogen). The digital images were captured using a fluorescence microscope BZ-X800 (Keyence). The image processing and quantitative analyses were performed using the ImageJ/Fiji software (NIH).

Statistical analysis

All statistical analyses were performed using GraphPad Prism or IBM SPSS Statistics. Datasets were first tested for outliers using the Grubb’s test, and then subjected to Shapiro–Wilk test of normality and Levene’s test of variance homogeneity. The Mann–Whitney *U* test and Kruskal–Wallis test were used for nonparametric tests, ANOVA were utilized for parametric tests, and $p < 0.05$ was considered statistically significant.

Results

Siglec-E is abundantly expressed in mouse primary microglia, and its knockdown by shRNA transformed microglia to a state displaying aggravated proinflammatory characteristics when exposed to neural debris, mimicking DAMPs [33]. A similar relation between Siglec-E and reactive microgliosis following the exposure to PAMPs was also reported, as CRISPR/Cas9-mediated Siglec-E knockout in microglial cell line BV2 resulted in a stronger response to LPS stimulation [34]. However, investigation on congenital ablation of Siglec-E in primary microglia has not been reported to date. For that, we first cultured the mouse primary brain microglia derived from C57BL/6 wild type and Siglec-E knockout pups. Immunostaining for the microglial marker Iba-1 revealed that the purity of microglia was about 95% in the wild-type cultures and 96% in the Siglec-E knockout cultures (Fig. 1A). We then stimulated these cells with LPS (0, 1, 10, or 100 ng/mL). After overnight treatment, a number of key proinflammatory mediators secreted by LPS-activated microglia into the culture medium were measured by ELISA. It was found that LPS induced prostaglandin E₂ (PGE₂, Fig. 1B) and prototypical proinflammatory cytokines IL-1 β (Fig. 1C), IL-6 (Fig. 1D),

and TNF- α (Fig. 1E) in both wild type and Siglec-E knockout microglia in a concentration-dependent manner. However, the levels of PGE₂ and cytokines were substantially higher in the Siglec-E knockout microglia when compared to the wild-type cells (Fig. 1B–E). These results demonstrate a key anti-inflammatory and immunosuppressive role for microglial Siglec-E in response to PAMPs like LPS.

The molecular mechanisms whereby the ablation of Siglec-E prevents the LPS-induced microglia-mediated inflammation is not fully understood. However, LPS induces inflammatory reactions via directly binding to the toll-like receptor 4 (TLR4), which is believed to be restrained by Siglec-E [44]. In the absence of Siglec-E, LPS-activated TLR4 is free to fully engage the downstream inflammatory mediators, although LPS may not directly act on Siglec-E. To further investigate the effects of LPS/TLR4-mediated inflammation on Siglec-E in vivo, we next examined the expression of Siglec-E in the brain after systemic treatment with LPS (3 or 5 mg/kg, i.p.) in adult C57BL/6 wild-type mice. It was found that LPS considerably induced mRNA expression of Siglec-E in the hippocampus in a dose-dependent manner, measured 24 h after the treatment (Fig. 2A). The induction of Siglec-E mRNA by LPS in wild-type mice and its absence in Siglec-E knockout mice were validated by reverse transcription PCR (Fig. 2B).

Interestingly, immunohistochemistry revealed a trend that, under basal conditions, the ablation of Siglec-E increased Iba1-positive (Iba1⁺) cells and the overall expression of Iba1 in the hippocampus (Fig. 2C), although the difference between the wild type and Siglec-E knockout mice was not statistically significant (Fig. 2D). The induction of Siglec-E by LPS in the brain tissues from wild-type mice was confirmed by immunohistochemistry, which also revealed considerable cellular colocalization between Siglec-E and microglial marker Iba1 in brain tissues from LPS-treated mice (Fig. 2C). Moreover, the LPS-induced reactive microgliosis featured by the increased Iba1⁺ cells and elevated expression of Iba1 in the brain was further enhanced in Siglec-E knockout mice when compared to the wild-type animals (Fig. 2D).

We then carried out the morphological analyses on Iba1⁺ brain microglia using 26 measurements by NIH

ImageJ/Fiji software (Table 1, <https://imagej.nih.gov/ij/docs/menus/analyze.html>) [49], and the normalized outcomes were shown in a radar chart (Fig. 3A). In addition, the principal component analyses were performed to illustrate the morphological changes of activated microglia upon the LPS treatment and deletion of Siglec-E (Fig. 3B). It appeared that the LPS-driven morphological alterations of microglia were largely augmented by the absence of functional Siglec-E (Fig. 3A, B). These findings together suggest that inducible Siglec-E plays an essential role in the regulation of microglial activation and that its depletion would exacerbate microgliosis within the brain exposed to PAMPs.

In addition to neuroinflammation triggered by various PAMPs, sterile injured brain tissues can release DAMPs to activate innate immune receptors particularly on microglia, which, in turn, drive inflammatory reactions in neurological conditions such as ischemic stroke [38]. The induction of Siglec-E expression in the brain following ischemic stroke was first reported in a recent transcriptome screening study and appeared dependent on GPR68, a neuronal metabotropic proton receptor that mediates neuroprotection in acidotic and ischemic conditions [50]. We thus hypothesize that the inducible Siglec-E might be involved in an intrinsic neuroprotective strategy of the brain following ischemic injury. To test this hypothesis, we first examined the effects of genetic ablation of Siglec-E on oxygen–glucose deprivation (OGD)-induced cell death in mouse primary cortical cultures containing both neurons and glial cells. Primary cortical cultures from wild type or Siglec-E knockout mouse embryos (E18) were exposed to OGD for 1.5, 3, and 4.5 h, followed by reoxygenation and complete nutrition supplement for 16 h. The cell viability was measured using MTT assay, and we found that OGD induced cell death in these mouse primary cortical cultures in a time-dependent manner. Intriguingly, the neuronal death caused by moderate (3 h) but not mild (1.5 h) or severe (4.5 h) OGD was significantly augmented in neuroglia mixed cortical cultures derived from Siglec-E knockout mice when compared to wild-type control cells (Fig. 4A).

Motivated by the promising neuroprotection of Siglec-E after moderate OGD, we next sought to determine the role of Siglec-E in ischemic injury in our mouse model of

(See figure on next page.)

Fig. 2 Ablation of Siglec-E exacerbates microglial activation in the brain. **A** C57BL/6 wild type and Siglec-E knockout mice were systemically treated by LPS (0, 3, or 5 mg/kg, i.p.), and 24 h later the mRNA expression of Siglec-E in the hippocampus was measured by qPCR ($n = 5-8$, $*p = 0.01$, Kruskal–Wallis test with post hoc Dunn's multiple comparisons). Data are visualized using box plot. **B** Reverse transcription PCR was performed to examine the Siglec-E mRNA expression in the hippocampal tissues of wild type and Siglec-E knockout mice treated by LPS, with GAPDH as control. **C** Immunostaining for Siglec-E (green fluorescence) and Iba1 (red fluorescence) indicating the hippocampal microglial activation in wild type and Siglec-E knockout mice was performed 24 h after LPS treatment (5 mg/kg, i.p.). Representative images are presented here to exemplify the induction of Siglec-E and Iba1 as well as their colocalization in activated microglia. Scale bar: 50 μm . **D** Iba1-positive (Iba1⁺) microglia in the hippocampus were counted (Left) and their Iba1 expression levels were quantified by measuring the fluorescence intensity (Right) ($n = 4-6$, $*p < 0.05$, $**p < 0.01$, Mann–Whitney U test). Data are shown as mean \pm SEM

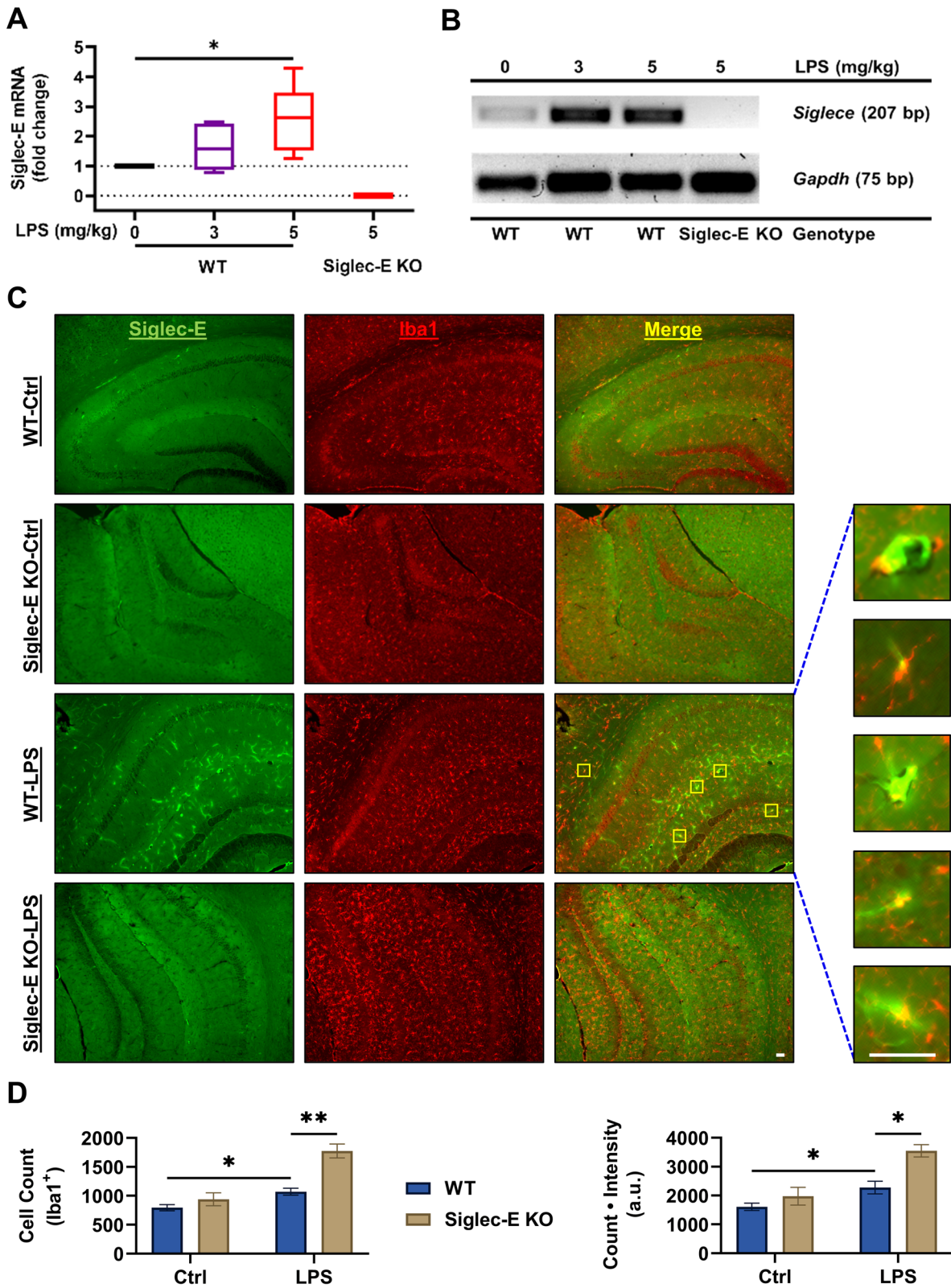


Fig. 2 (See legend on previous page.)

Table 1 The 26 measurements that are used to characterize the microglial morphology

| Measurement | Definition |
|-----------------------|---|
| Kurtosis | The fourth-order moment about the mean |
| Min. gray level | Minimum gray values within the selection |
| Median | The median value of the pixels in the image or selection |
| Modal gray value | Most frequently occurring gray value within the selection |
| Mean gray value | Average gray value within the selection |
| Circularity | $= 4\pi \times \text{area}/\text{perimeter}^2$ |
| Solidity | $= \text{Area}/\text{convex area}$ |
| Max. gray level | Maximum gray values within the selection |
| Roundness | $= 4 \times \text{area}/(\pi \times \text{major_axis}^2)$, or the inverse of the aspect ratio |
| Average branch length | The average length of branches, in the corresponding units |
| Aspect ratio | $= \text{major_axis}/\text{minor_axis}$ |
| Standard deviation | Standard deviation of the gray values |
| Maximum branch length | The maximum length of branches, in the corresponding units |
| MinFeret | The minimum caliper diameter |
| Feret's diameter | The longest distance between any two points along the selection boundary |
| Integrated density | The product of area and mean gray value |
| Perimeter | The length of the outside boundary of the selection |
| End-point pixels | Count of pixels if they have less than 2 neighbors |
| Area | Area of selection in square pixels |
| Skewness | The third order moment about the mean |
| Branches | The number of branches |
| Slab pixels | Count of pixels if they have exactly 2 neighbors |
| Quadruple points | The number of triple points |
| Triple points | The number of quadruple points |
| Junctions | The number of actual junctions |
| Junction pixels | Count of pixels if they have more than 2 neighbors |

More detailed information about these measurements can be found from <https://imagej.nih.gov/ij/docs/menus/analyze.html> and [49]

(See figure on next page.)

Fig. 3 Siglec-E regulates the morphology of brain microglia. **A** The morphological analyses of brain microglia (Iba1⁺) in mice with 26 measurements (Table 1) were performed 24 h after LPS treatment (5 mg/kg, i.p.) using ImageJ/Fiji software. A radar chart was generated to show the morphological changes of brain microglia in mice by LPS treatment and deletion of Siglec-E. The statistical p values less than 0.1 were labeled ($n = 4-6$, $*p < 0.05$, $**p < 0.01$, Mann-Whitney U test). Note that the 26 measurements can be categorized into three clusters indicated by purple, green, and yellow arcs, showing that the measurements in wild-type control mice, when compared to other two groups, were higher, equivalent, and lower, respectively. **B** Principal component analysis of microglial morphology was performed using IBM SPSS Statistics software with 3000 microglia randomly sampled from each group. The observable core cluster of brain microglia in wild-type control group (black dots) is shown by an ellipse (~90%). The remaining cells were scattered either along the positive axis of principal component 1 (~6%) or along the negative axis of principal component 2 (~4%). Treatment with LPS (blue dots) increased the cells scattered out of the core to ~17%, which was further increased in LPS-treated Siglec-E knockout mice (red dots) to ~25%

transient brain ischemia, in which middle cerebral artery occlusion (MCAO) lasts for about 30 min and is followed by reperfusion for 72 h (Fig. 4B). We first validated the significant induction of Siglec-E expression within the ipsilateral hemisphere of wild-type mice by a 30-min episode of MCAO when compared to the sham control (Fig. 4C), suggesting that a moderate transient brain ischemia was able to induce Siglec-E in the ischemic

brain regions. We then found that the genetic ablation of Siglec-E led to more severe neurological deficits measured by Bederson scale during the 72-h reperfusion (Fig. 4D). Likewise, the Siglec-E knockout mice overall experienced higher post-stroke weight loss when compared to the wild-type control animals (Fig. 4E). Intriguingly, the neurological deficits of both wild type and Siglec-E knockout mice appeared to stabilize since 24 h

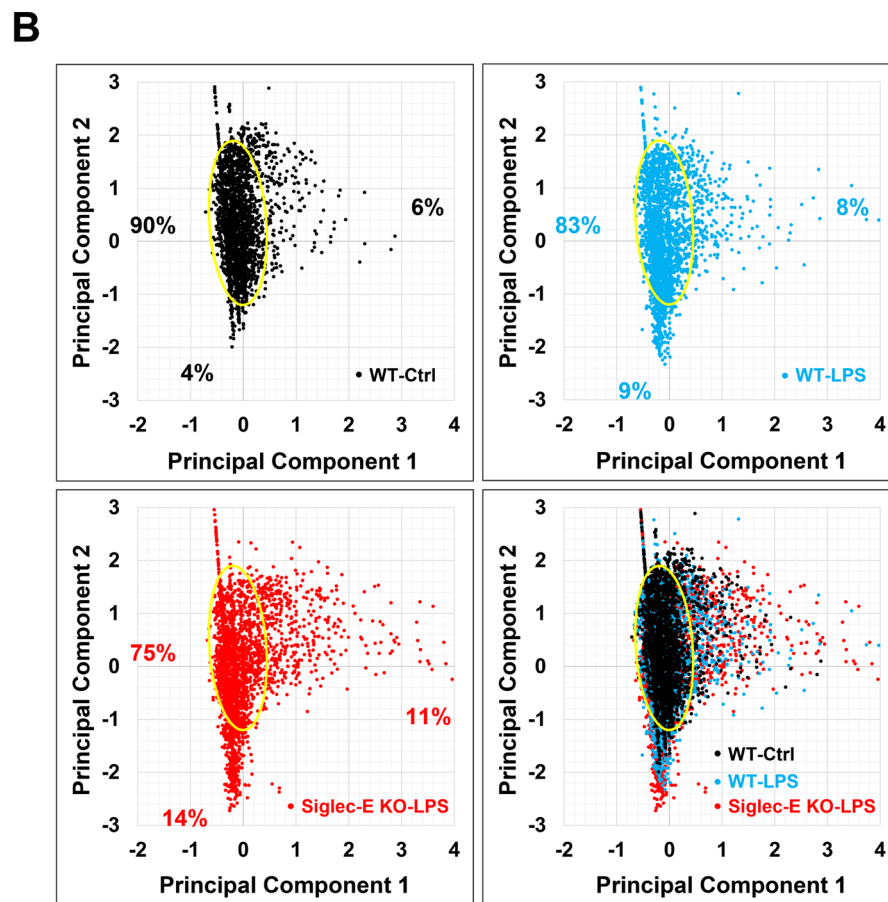
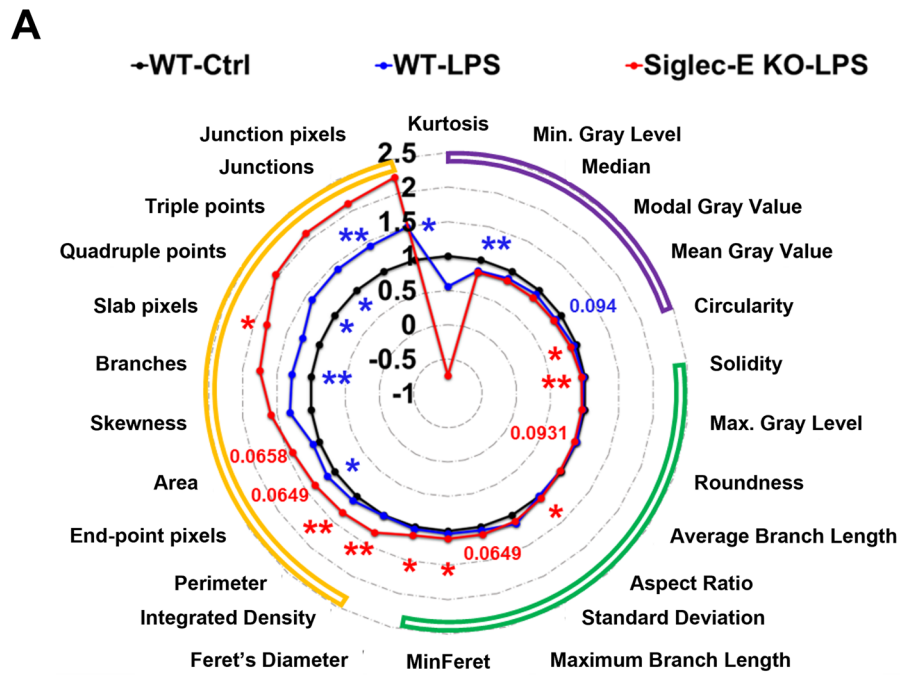


Fig. 3 (See legend on previous page.)

after MCAO (Fig. 4D), whereas their weight loss continued throughout the experimental period (Fig. 4E). The observation that more weight loss was not necessarily associated with severer neurological deficits suggests that the assessment of neurological deficits by Bederson scale was unlikely interfered by the concomitant weight loss.

A 30-min episode of MCAO was sufficient to cause moderate brain damages in wild-type mice, indicated by medium-sized brain infarcts ($\sim 20 \text{ mm}^3$) found in the cortex and striatum (Fig. 4F). In line with the worsened post-stroke wellbeing in Siglec-E knockout mice, the MCAO-triggered brain damages were exacerbated by the genetic deletion of Siglec-E, as the brain infarct volumes were nearly doubled in Siglec-E knockout mice when compared to the wild-type cohort (Fig. 4G). However, the ablation of Siglec-E did not significantly alter the post-stroke mortality rates in mice (Fig. 4H). Nonetheless, these post-stroke outcomes together support a neuroprotective role of induced Siglec-E following ischemic stroke.

Discussion

Activation of Siglec-E by sialic acid-containing glycans has been increasingly recognized as a critical immunosuppressive mechanism in response to various PAMPs and DAMPs. The expression of Siglec-E is low in the naïve brain, but with inflammatory or injurious stimulation it is rapidly and robustly induced, particularly in microglia. In this study, we found that the genetic ablation of Siglec-E led to a vigorous increase of the LPS response of microglia both in vitro and in vivo. The Siglec-E deficiency also aggravated OGD-triggered neuronal death in mouse primary cortical neuron–glia mixed cultures and augmented ischemic brain injury in mice. These new findings demonstrate profound anti-inflammatory and neuroprotective functions of induced Siglec-E following exposure of the brain to PAMPs or DAMPs. As such, the current study provides the *first* indication of an intrinsic self-protection mechanism of the brain for

inflammation resolution and tissue repair after ischemic stroke or other acute neurological insults.

The mouse ENCODE transcriptome data (<https://www.ncbi.nlm.nih.gov/gene/83382>) suggest that Siglec-E is most abundantly expressed in the adult spleen [51]. In the CNS, the Allen Mouse Brain Atlas has reported that the expression of Siglec-E is mainly enriched in olfactory bulb, hippocampus, neocortical layer II, and cerebellum (<http://mouse.brain-map.org/gene/show/57631>). Although the basal expression of Siglec-E in the brain is overall low, it can be rapidly and robustly induced by various injurious and inflammatory stimuli. In this study, we found that Siglec-E was markedly upregulated under both PAMPs and DAMPs-related disease conditions. In particular, the upregulated Siglec-E showed colocalization with microglial marker Iba1 in the brain after LPS treatment in mice, suggesting that microglia are a major cellular source for Siglec-E expression in brain upon challenges. Intriguingly, the elevated Siglec-E appeared to diminish the surge of proinflammatory mediators produced by microglia, reduce the number of microglia, and counteract their morphological changes when they are activated. As such, Siglec-E likely plays a preventive role in the microglial transformation from resting state to activated state. However, it should be noted that an evident portion of the Siglec-E was detected in cells that did not express Iba1 (Iba-1^-), indicating that microglia may not be the only type of cells expressing Siglec-E in the brain responding to inflammatory challenges. Likewise, microglia may not be the only brain-resident immunoreactive cells expressing Siglec-E upon LPS stimulation or ischemic injury, as peripheral Iba-1^+ myeloid cells can infiltrate into the brain parenchyma under these conditions. Future investigation using cell type-specific knockout strategies is needed to identify all these Siglec-E-expressing cells (Iba-1^+ or Iba-1^-) in the brain in order to fully understand the roles of Siglec-E in health and disease.

(See figure on next page.)

Fig. 4 Induced Siglec-E is neuroprotective after ischemia–reperfusion injuries. **A** Primary neuron–glia cultures derived from cortices of wild type or Siglec-E knockout mouse embryos were subjected to oxygen–glucose deprivation (OGD) for 1.5, 3, or 4.5 h. Following reoxygenation with full nutrition supply for 16 h, the cell viability in these cultures was measured and compared ($n = 8–24$, $*p = 0.0172$, two-way ANOVA with post hoc Šidák multiple comparisons). Data are presented as mean \pm SEM. **B** Intraluminal filament-based middle cerebral artery occlusion (MCAO) model was utilized to examine the effects of genetic ablation of Siglec-E on cerebral ischemia. In this study, adult wild type and Siglec-E knockout male mice (12–14 weeks old) were subjected to transient MCAO for 30 min, which was followed by reperfusion for 72 h. **C** Siglec-E mRNA expression in the ipsilateral brain tissues of mice subjected to 30-min MCAO and 72-h reperfusion was measured by qPCR and compared to that of sham cohort ($n = 7–14$, $***p < 0.0001$, Mann–Whitney U test). Data are visualized using box plot. **D** Neurological deficits of wild type and Siglec-E knockout mice after MCAO were evaluated at multiple time points using Bederson's scale ($n = 12–16$, $***p < 0.001$, two-way ANOVA). Data are presented as mean \pm SEM. **E** Deficiency of Siglec-E in mice exacerbated post-stroke weight loss ($n = 12–16$, $***p < 0.001$, two-way ANOVA with post hoc Šidák multiple comparisons). Data are presented as mean \pm SEM. **F** Triphenyltetrazolium chloride (TTC) staining was performed to measure the brain infarction in wild type and Siglec-E knockout mice 72 h after MCAO. Representative images from each cohort are shown. The viable brain parenchyma appeared reddish, whereas the infarcted areas were pale and highlighted. **G** The volumes of brain infarcts in wild type and Siglec-E knockout mice were quantified and compared ($n = 10–14$, $*p = 0.022$, Mann–Whitney U test). Data are presented as mean \pm SEM. **H** Animal mortality over 72 h following transient MCAO for 30 min ($n = 14–17$, $p = 0.5734$, log-rank test)

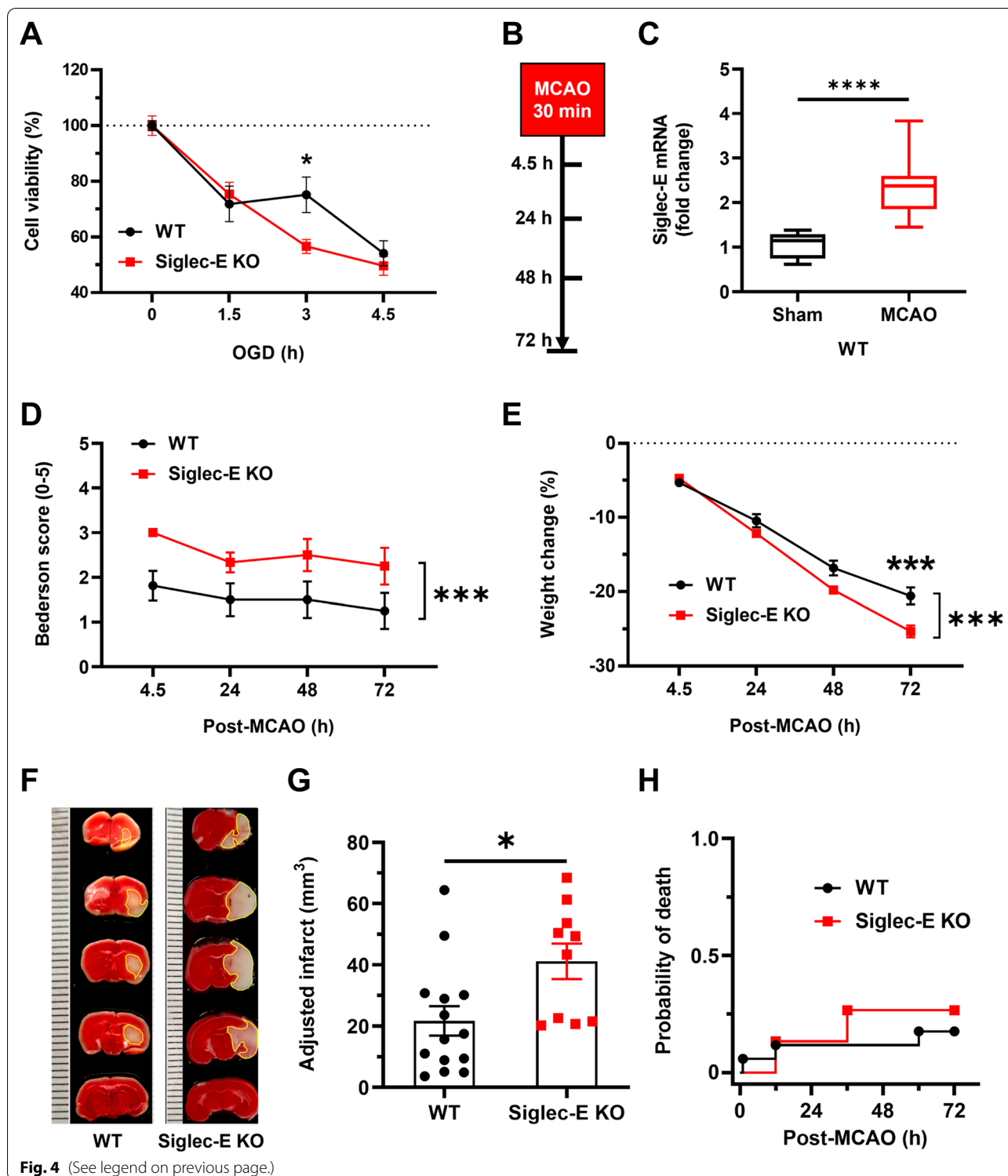


Fig. 4 (See legend on previous page.)

Excessive reactive microgliosis is sufficient to cause neuronal damage and is considered pro-neurodegenerative, as the activation of some pattern recognition receptors expressed on the microglial surface often leads

to the release of reactive oxygen species (ROS) that can trigger neurotoxicity [52]. Conversely, as another type of pattern recognition receptors expressed by microglia, Siglec-E overall is immunosuppressive, and it functions

against reactive microgliosis. Previous evidence supports the notion that microglial Siglec-E is neuroprotective through attenuating neuroinflammation and phagocytosis-associated oxidative stress [33, 53]. Microglial Siglec-E was shown to prevent neurotoxicity through interacting with the sialic acid decorated on the neuronal glycocalyx [53]. In line with this, our findings support anti-inflammatory and neuroprotective roles of Siglec-E after ischemic stroke. Thus, pharmacological activation of Siglec-E may trigger the ITIM-mediated intracellular immunoinhibitory signaling and predispose activated myeloid immunocytes to a quiescent state. Future studies should also be directed to identify therapeutic agents that can directly activate Siglec-E. For instance, pS9L-lipid, a glycopolypeptide ligand as a *cis*-binding agonist for Siglec-E and Siglec-9 (the human ortholog of mouse Siglec-E), can inhibit TLR4-induced NF- κ B activity, MAPK signaling, and phagocytosis by macrophages and microglia [54], demonstrating *cis*-binding agonists as a way to activate Siglecs in inflammatory diseases. Whether these *cis* ligands can cross the blood–brain barrier and be useful to suppress post-stroke neuroinflammation following brain insults such as ischemic stroke is another interesting question that remains to be answered. Similarly, selective sialidase inhibitors, which aim to increase the Siglec-E activity and suppress inflammatory response [44, 55], should also be tested in animal models of MCAO for potential use in stroke treatment.

In sum, our findings indicate that the Siglec-E in microglia is rapidly induced by LPS and ischemic stroke and, in turn, leads to beneficial, anti-inflammatory, and neuroprotective effects under these neuroinflammatory conditions. This suggests that Siglec-E activation by selective agonists might represent a novel immunomodulatory strategy to confer neuroprotection in cerebral ischemia and other acute or chronic neurological conditions in which neuroinflammation facilitates neuronal death.

Abbreviations

DAMPs: Damage-associated molecular patterns; DAP12: DNAX-activating protein of 12 kDa; ITAM: Immunoreceptor tyrosine-based activation motif; ITIM: Immunoreceptor tyrosine-based inhibitory motif; KARAP: Killer cell activating receptor-associated protein; LPS: Lipopolysaccharide; MAPK: Mitogen-activated protein kinase; MCAO: Middle cerebral artery occlusion; NF- κ B: Nuclear factor κ B; OGD: Oxygen–glucose deprivation; PAMPs: Pathogen-associated molecular patterns; ROS: Reactive oxygen species; Siglec-E: Sialic acid immunoglobulin-like lectin E; TBI: Traumatic brain injury; TLR4: Toll-like receptor 4; TYROBP: Tyrosine kinases binding protein.

Acknowledgements

Not applicable.

Author contributions

LL, YC, JH, YW, GYC, YY, and JJ designed the study. LL, YC, MNS, and RH conducted the experiments. LL, YC, MNS, YY, and JJ processed, analyzed, and interpreted the results. LL, YC, YY, and JJ wrote the manuscript. All authors

reviewed and approved the final manuscript. All authors read and approved the final manuscript.

Funding

This work was supported by the National Institutes of Health (NIH) Grants R01NS100947 (J.J.), R21NS109687 (J.J.), R61NS124923 (J.J.), R01NS105787 (J.H.), and R01AI137255 (G.Y.C.).

Availability of data and materials

All relevant data in this study are available upon reasonable request directed to the corresponding author.

Declarations

Competing interests

The authors declare no competing interests.

Ethics approval and consent to participate

The animal experiments and procedures were approved by the Institutional Animal Care and Use Committee (IACUC) of the University of Tennessee Health Science Center and carried out in accordance with the *Guide for the Care and Use of Laboratory Animals* (the *Guide*) from the NIH.

Consent for publication

Not applicable.

Competing interests

The authors declare that they have no competing interests.

Author details

¹Department of Pharmaceutical Sciences, Drug Discovery Center, College of Pharmacy, University of Tennessee Health Science Center, Memphis, TN, USA. ²Department of Pharmacological and Pharmaceutical Sciences, College of Pharmacy, University of Houston, Houston, TX, USA. ³Children's Foundation Research Institute at Le Bonheur Children's Hospital, Department of Pediatrics, College of Medicine, University of Tennessee Health Science Center, Memphis, TN, USA.

Received: 15 April 2022 Accepted: 14 July 2022

Published online: 20 July 2022

References

- Varki A, Schnaar RL, Crocker PR, et al. I-type lectins. In: Varki A, Cummings RD, Esko JD, Stanley P, Hart GW, Aebi M, Darvill AG, Kinoshita T, Packer NH, Prestegard JH, et al., editors. *Essentials of glycobiology*. 3rd ed. La Jolla: Cold Spring Harbor Laboratory Press; 2015. p. 453–67. <https://doi.org/10.1101/glycobiology.3e.035>.
- Crocker PR, Paulson JC, Varki A. Siglecs and their roles in the immune system. *Nat Rev Immunol*. 2007;7:255–66. <https://doi.org/10.1038/nri2056>.
- Laubli H, Varki A. Sialic acid-binding immunoglobulin-like lectins (Siglecs) detect self-associated molecular patterns to regulate immune responses. *Cell Mol Life Sci*. 2020;77:593–605. <https://doi.org/10.1007/s00018-019-03288-x>.
- Ulyanova T, Shah DD, Thomas ML. Molecular cloning of MIS, a myeloid inhibitory siglec, that binds protein-tyrosine phosphatases SHP-1 and SHP-2. *J Biol Chem*. 2001;276:14451–8. <https://doi.org/10.1074/jbc.M011650200>.
- Tomioka Y, Morimatsu M, Nishijima K, Usui T, Yamamoto S, Suyama H, et al. A soluble form of Siglec-9 provides an antitumor benefit against mammary tumor cells expressing MUC1 in transgenic mice. *Biochem Biophys Res Commun*. 2014;450:532–7. <https://doi.org/10.1016/j.bbrc.2014.06.009>.
- Laubli H, Alisson-Silva F, Stanczak MA, Siddiqui SS, Deng L, Verhagen A, et al. Lectin galactoside-binding soluble 3 binding protein (LGALS3BP) is a tumor-associated immunomodulatory ligand for CD33-related Siglecs. *J Biol Chem*. 2014;289:33481–91. <https://doi.org/10.1074/jbc.M114.593129>.

7. Laubli H, Pearce OM, Schwarz F, Siddiqui SS, Deng L, Stanczak MA, et al. Engagement of myelomonocytic Siglecs by tumor-associated ligands modulates the innate immune response to cancer. *Proc Natl Acad Sci U S A*. 2014;111:14211–6. <https://doi.org/10.1073/pnas.1409580111>.
8. Wielgat P, Czarnomysy R, Trofimiuk E, Car H. The sialoglycan-Siglec-E checkpoint axis in dexamethasone-induced immune subversion in glioma-microglia transwell co-culture system. *Immunol Res*. 2019;67:348–57. <https://doi.org/10.1007/s12026-019-09106-7>.
9. Gray MA, Stanczak MA, Mantuano NR, Xiao H, Pijnenborg JFA, Malaker SA, et al. Targeted glycan degradation potentiates the anticancer immune response in vivo. *Nat Chem Biol*. 2020;16:1376–84. <https://doi.org/10.1038/s41589-020-0622-x>.
10. Friedman DJ, Crotts SB, Shapiro MJ, Rajcula M, McCue S, Liu X, et al. ST8Sia6 promotes tumor growth in mice by inhibiting immune responses. *Cancer Immunol Res*. 2021;9:952–66. <https://doi.org/10.1158/2326-6066.CCR-20-0834>.
11. Ibarlucea-Benitez I, Weitzenfeld P, Smith P, Ravetch JV. Siglecs-7/9 function as inhibitory immune checkpoints in vivo and can be targeted to enhance therapeutic antitumor immunity. *Proc Natl Acad Sci U S A*. 2021. <https://doi.org/10.1073/pnas.2107424118>.
12. Erdmann H, Steeg C, Koch-Nolte F, Fleischer B, Jacobs T. Sialylated ligands on pathogenic *Trypanosoma cruzi* interact with Siglec-E (sialic acid-binding Ig-like lectin-E). *Cell Microbiol*. 2009;11:1600–11. <https://doi.org/10.1111/j.1462-5822.2009.01350.x>.
13. Ferrero MR, Heins AM, Soprano LL, Acosta DM, Esteva MI, Jacobs T, et al. Involvement of sulfates from cruzipain, a major antigen of *Trypanosoma cruzi*, in the interaction with immunomodulatory molecule Siglec-E. *Med Microbiol Immunol*. 2016;205:21–35. <https://doi.org/10.1007/s00430-015-0421-2>.
14. Palus M, Sohrabi Y, Broman KW, Strnad H, Sima M, Ruzek D, et al. A novel locus on mouse chromosome 7 that influences survival after infection with tick-borne encephalitis virus. *BMC Neurosci*. 2018;19:39. <https://doi.org/10.1186/s12868-018-0438-8>.
15. Karmakar J, Mandal C. Interplay between sialic acids, Siglec-E, and Neu1 regulates MyD88- and TRIF-dependent pathways for TLR4-activation during *Leishmania donovani* infection. *Front Immunol*. 2021;12: 626110. <https://doi.org/10.3389/fimmu.2021.626110>.
16. Chang YC, Olson J, Beasley FC, Tung C, Zhang J, Crocker PR, et al. Group B *Streptococcus* engages an inhibitory Siglec through sialic acid mimicry to blunt innate immune and inflammatory responses in vivo. *PLoS Pathog*. 2014;10: e1003846. <https://doi.org/10.1371/journal.ppat.1003846>.
17. Wu Y, Ren D, Chen GY. Siglec-E negatively regulates the activation of TLR4 by controlling its endocytosis. *J Immunol*. 2016;197:3336–47. <https://doi.org/10.4049/jimmunol.1600772>.
18. Nagala M, McKenzie E, Richards H, Sharma R, Thomson S, Mastroeni P, et al. Expression of Siglec-E alters the proteome of lipopolysaccharide (LPS)-activated macrophages but does not affect LPS-driven cytokine production or toll-like receptor 4 endocytosis. *Front Immunol*. 2017;8:1926. <https://doi.org/10.3389/fimmu.2017.01926>.
19. Patras KA, Coady A, Olson J, Ali SR, RamachandraRao SP, Kumar S, et al. Tamm-Horsfall glycoprotein engages human Siglec-9 to modulate neutrophil activation in the urinary tract. *Immunol Cell Biol*. 2017;95:960–5. <https://doi.org/10.1038/icb.2017.63>.
20. Uchiyama S, Sun J, Fukahori K, Ando N, Wu M, Schwarz F, et al. Dual actions of group B *Streptococcus* capsular sialic acid provide resistance to platelet-mediated antimicrobial killing. *Proc Natl Acad Sci U S A*. 2019;116:7465–70. <https://doi.org/10.1073/pnas.1815572116>.
21. Liu H, Zheng Y, Zhang Y, Li J, Fernandes SM, Zeng D, et al. Immunosuppressive Siglec-E ligands on mouse aorta are up-regulated by LPS via NF-kappaB pathway. *Biomed Pharmacother*. 2020;122: 109760. <https://doi.org/10.1016/j.biopha.2019.109760>.
22. Wu Y, Yang D, Liu R, Wang L, Chen GY. Selective response to bacterial infection by regulating Siglec-E expression. *iScience*. 2020;23:101473. <https://doi.org/10.1016/j.isci.2020.101473>.
23. McMillan SJ, Sharma RS, McKenzie EJ, Richards HE, Zhang J, Prescott A, et al. Siglec-E is a negative regulator of acute pulmonary neutrophil inflammation and suppresses CD11b beta2-integrin-dependent signaling. *Blood*. 2013;121:2084–94. <https://doi.org/10.1182/blood-2012-08-449983>.
24. McMillan SJ, Sharma RS, Richards HE, Hegde V, Crocker PR. Siglec-E promotes beta2-integrin-dependent NADPH oxidase activation to suppress neutrophil recruitment to the lung. *J Biol Chem*. 2014;289:20370–6. <https://doi.org/10.1074/jbc.M114.574624>.
25. Mukherjee K, Khatua B, Mandal C. Sialic acid-Siglec-E interactions during *Pseudomonas aeruginosa* infection of macrophages interferes with phagosomal maturation by altering intracellular calcium concentrations. *Front Immunol*. 2020;11:332. <https://doi.org/10.3389/fimmu.2020.00332>.
26. Chen Z, Xu SL, Ge LY, Zhu J, Zheng T, Zhu Z, et al. Sialic acid-binding immunoglobulin-like lectin 9 as a potential therapeutic target for chronic obstructive pulmonary disease. *Chin Med J (Engl)*. 2021;134:757–64. <https://doi.org/10.1097/CM9.0000000000001381>.
27. Yu H, Gonzalez-Gil A, Wei Y, Fernandes SM, Porell RN, Vajn K, et al. Siglec-8 and Siglec-9 binding specificities and endogenous airway ligand distributions and properties. *Glycobiology*. 2017;27:657–68. <https://doi.org/10.1093/glycob/cwx026>.
28. Chen Z, Bai FF, Han L, Zhu J, Zheng T, Zhu Z, et al. Targeting neutrophils in severe asthma via Siglec-9. *Int Arch Allergy Immunol*. 2018;175:5–15. <https://doi.org/10.1159/000484873>.
29. Hsu YW, Hsu FF, Chiang MT, Tsai DL, Li FA, Angata T, et al. Siglec-E retards atherosclerosis by inhibiting CD36-mediated foam cell formation. *J Biomed Sci*. 2021;28:5. <https://doi.org/10.1186/s12929-020-00698-z>.
30. Zhang Y, Zheng Y, Li J, Nie L, Hu Y, Wang F, et al. Immunoregulatory Siglec ligands are abundant in human and mouse aorta and are up-regulated by high glucose. *Life Sci*. 2019;216:189–99. <https://doi.org/10.1016/j.lfs.2018.11.049>.
31. Belmonte PJ, Shapiro MJ, Rajcula MJ, McCue SA, Shapiro VS. Cutting edge: ST8Sia6-generated alpha-2,8-disialic acids mitigate hyperglycemia in multiple low-dose streptozotocin-induced diabetes. *J Immunol*. 2020;204:3071–6. <https://doi.org/10.4049/jimmunol.2000023>.
32. Flores R, Zhang P, Wu W, Wang X, Ye P, Zheng P, et al. Siglec genes confer resistance to systemic lupus erythematosus in humans and mice. *Cell Mol Immunol*. 2019;16:154–64. <https://doi.org/10.1038/cmi.2017.160>.
33. Claude J, Linnartz-Gerlach B, Kudin AP, Kunz WS, Neumann H. Microglial CD33-related Siglec-E inhibits neurotoxicity by preventing the phagocytosis-associated oxidative burst. *J Neurosci*. 2013;33:18270–6. <https://doi.org/10.1523/JNEUROSCI.2211-13.2013>.
34. Thiesler H, Beimdiek J, Hildebrandt H. Polysialic acid and Siglec-E orchestrate negative feedback regulation of microglia activation. *Cell Mol Life Sci*. 2021;78:1637–53. <https://doi.org/10.1007/s00018-020-03601-z>.
35. Greter M, Lelios I, Croxford AL. Microglia versus myeloid cell nomenclature during brain inflammation. *Front Immunol*. 2015;6:249. <https://doi.org/10.3389/fimmu.2015.00249>.
36. Li D, Lang W, Zhou C, Wu C, Zhang F, Liu Q, et al. Upregulation of microglial ZEB1 ameliorates brain damage after acute ischemic stroke. *Cell Rep*. 2018;22:3574–86. <https://doi.org/10.1016/j.celrep.2018.03.011>.
37. Jayaraj RL, Azimullah S, Beiram R, Jalal FY, Rosenberg GA. Neuroinflammation: friend and foe for ischemic stroke. *J Neuroinflammation*. 2019;16:142. <https://doi.org/10.1186/s12974-019-1516-2>.
38. Iadecola C, Buckwalter MS, Anrather J. Immune responses to stroke: mechanisms, modulation, and therapeutic potential. *J Clin Invest*. 2020;130:2777–88. <https://doi.org/10.1172/JCI135530>.
39. Xu X, Du L, Jiang J, Yang M, Wang Z, Wang Y, et al. Microglial TREM2 mitigates inflammatory responses and neuronal apoptosis in angiotensin II-induced hypertension in middle-aged mice. *Front Aging Neurosci*. 2021;13: 716917. <https://doi.org/10.3389/fnagi.2021.716917>.
40. Li L, Yasmen N, Hou R, Yang S, Lee JY, Hao J, et al. Inducible prostaglandin E synthase as a pharmacological target for ischemic stroke. *Neurotherapeutics*. 2022;19:366–85. <https://doi.org/10.1007/s13311-022-01191-1>.
41. Li L, Yu Y, Hou R, Hao J, Jiang J. Inhibiting the PGE2 receptor EP2 mitigates excitotoxicity and ischemic injury. *ACS Pharmacol Transl Sci*. 2020;3:635–43. <https://doi.org/10.1021/acspsci.0c00040>.
42. Yu Y, Li L, Nguyen DT, Mustafa SM, Moore BM, Jiang J. Inverse agonism of cannabinoid receptor type 2 confers anti-inflammatory and neuroprotective effects following status epilepticus. *Mol Neurobiol*. 2020;57:2830–45. <https://doi.org/10.1007/s12035-020-01923-4>.
43. Fu H, Wang J, Wang J, Liu L, Jiang J, Hao J. 4R-cembranoid protects neuronal cells from oxygen-glucose deprivation by modulating microglial cell activation. *Brain Res Bull*. 2022;179:74–82. <https://doi.org/10.1016/j.brainresbull.2021.12.007>.
44. Chen GY, Brown NK, Wu W, Khedri Z, Yu H, Chen X, et al. Broad and direct interaction between TLR and Siglec families of pattern recognition

- receptors and its regulation by Neu1. *Elife*. 2014;3: e04066. <https://doi.org/10.7554/eLife.04066>.
45. Xu X, Zhang C, Jiang J, Xin M, Hao J. Effect of TDP43-CTFs35 on brain endothelial cell functions in cerebral ischemic injury. *Mol Neurobiol*. 2022;59:4593–611. <https://doi.org/10.1007/s12035-022-02869-5>.
 46. Zhang C, Sajith AM, Xu X, Jiang J, Phillip Bowen J, Kulkarni A, et al. Targeting NLRP3 signaling by a novel-designed sulfonyleurea compound for inhibition of microglial inflammation. *Bioorg Med Chem*. 2022;58: 116645. <https://doi.org/10.1016/j.bmc.2022.116645>.
 47. Jiang J, Yu Y, Kinjo ER, Du Y, Nguyen HP, Dingledine R. Suppressing pro-inflammatory prostaglandin signaling attenuates excitotoxicity-associated neuronal inflammation and injury. *Neuropharmacology*. 2019;149:149–60. <https://doi.org/10.1016/j.neuropharm.2019.02.011>.
 48. Hou R, Yu Y, Sluter MN, Li L, Hao J, Fang J, et al. Targeting EP2 receptor with multifaceted mechanisms for high-risk neuroblastoma. *Cell Rep*. 2022;39: 111000. <https://doi.org/10.1016/j.celrep.2022.111000>.
 49. Arganda-Carreras I, Fernandez-Gonzalez R, Munoz-Barrutia A, Ortiz-De-Solorzano C. 3D reconstruction of histological sections: application to mammary gland tissue. *Microsc Res Tech*. 2010;73:1019–29. <https://doi.org/10.1002/jemt.20829>.
 50. Zhou G, Wang T, Zha XM. RNA-Seq analysis of knocking out the neuro-protective proton-sensitive GPR68 on basal and acute ischemia-induced transcriptome changes and signaling in mouse brain. *FASEB J*. 2021;35: e21461. <https://doi.org/10.1096/fj.202002511R>.
 51. Yue F, Cheng Y, Breschi A, Vierstra J, Wu W, Ryba T, et al. A comparative encyclopedia of DNA elements in the mouse genome. *Nature*. 2014;515:355–64. <https://doi.org/10.1038/nature13992>.
 52. Block ML, Zecca L, Hong JS. Microglia-mediated neurotoxicity: uncovering the molecular mechanisms. *Nat Rev Neurosci*. 2007;8:57–69. <https://doi.org/10.1038/nrn2038>.
 53. Linnartz-Gerlach B, Kopatz J, Neumann H. Siglec functions of microglia. *Glycobiology*. 2014;24:794–9. <https://doi.org/10.1093/glycob/cwu044>.
 54. Delaveris CS, Chiu SH, Riley NM, Bertozzi CR. Modulation of immune cell reactivity with cis-binding Siglec agonists. *Proc Natl Acad Sci U S A*. 2021. <https://doi.org/10.1073/pnas.2012408118>.
 55. Chen GY, Chen X, King S, Cavassani KA, Cheng J, Zheng X, et al. Amelioration of sepsis by inhibiting sialidase-mediated disruption of the CD24-SiglecG interaction. *Nat Biotechnol*. 2011;29:428–35. <https://doi.org/10.1038/nbt.1846>.

Publisher's Note

Springer Nature remains neutral with regard to jurisdictional claims in published maps and institutional affiliations.

Ready to submit your research? Choose BMC and benefit from:

- fast, convenient online submission
- thorough peer review by experienced researchers in your field
- rapid publication on acceptance
- support for research data, including large and complex data types
- gold Open Access which fosters wider collaboration and increased citations
- maximum visibility for your research: over 100M website views per year

At BMC, research is always in progress.

Learn more biomedcentral.com/submissions

